International Journal of Engineering Research & Technology (IJERT)
ISSN: 2278-0181
Vol. 10 Issue 05, May-2021

Swarm Particle Intelligence for Voltage Collapse Studies in Nigerian 330-Kv Power Network

Idoniboyeobu D. C[1], Ahiakwo C. O[2], Braide S. L[3], Idachaba Alexander O[4],
[1,2,3,4,]Department of Electrical and Electronics Engineering, Rivers State University,
Port Harcourt, Nigeria

Abstract: **This research reports the use of a Predictive Swarm Particle Intelligence (PSPI) for the study of the Nigerian 330-kV 34 bus power system. The PSPI technique is based on a neural machine intelligence technique that follows from auditory sensation in the brain and an evolutionary technique that follows from the organization of swarming particles. The combined effect is used to determine the critical and most critical lines within the power network after being subjected to overloading faults. Using the proposed approach in voltage collapse studies shows significant implications for power system operators and managers.**

Keywords: Auditory Processing, Neural Machine Intelligence, Power Networks, Swarm Intelligence, Voltage Collapse.

I. INTRODUCTION

Presently, the Nigerian power system's state shows that some regions within the more extensive high voltage power system network still experience incessant blackouts. In certain instances, when power is available, there is a very high likelihood that a blackout may occur. In most cases, the timely determination of when the blackout situation occurs is largely unknown in the field. Thus, to overcome this lapse, power system managers should employ highly accurate and timely prediction techniques to facilitate the process.

Another challenge is how best to implement voltage collapse detection/prediction solutions that can be useful as a mitigation scheme near real-time. This is indeed a challenging problem that requires the determination of optimal points for each new collapse scenario presented.

Existing back-propagation trained neuro-swarm techniques are useful predictive optimizers, but in-depth analysis of such techniques have revealed their inherent code complexity coupled with very little or no connection to biology and recent neuroscience discoveries - see, for instance, the recent argument in Hole and Ahmad (Hole & Ahmad, 2019). Another obvious challenge is that of real-time integration of the existing computational techniques in real power transmission systems in the context of smart grids.

In light of the challenges mentioned above, this research study aims to propose a suitable scheme and useful framework that is adaptive and accurate enough to secure the Nigerian power system network.

II. RELATED WORKS

Several research works abound in voltage stability, which defines several Voltage Stability Margins (VSMs) for use with standardized power system networks. In this research, a focus on the Voltage Collapse Index (VCI) which describes the state of security of the power system in the presence of a possible severe contingency, is considered.

Some of such related works can be found in (Prasad et al., 2020), where the concept of reactive power margins has been utilized in a functional link Artificial Neural Network (FLANN) to predict post-outage bus voltages after a series of voltage contingency selections. In their proposed model, an Artificial Neural Network (ANN) is used to predict the voltages in IEEE 14-bus power system considering different line outages and loading conditions. In contrast, fuzzy logic is used for contingency ranking of the predicted responses. Fuzzy Logic (FL) reduces the misranking effect observed from the conventional bus-voltage Performance Index (PI) using discrete linguistic data mappings. Their voltage collapse performance indices consider both voltage stability margin (VSM) and voltage deviation (VD) which used a technique earlier proposed in (Dobson & Lu, 1993). A set of 200 patterns have been used for neural training while 20 separate patterns are used for testing. Simulation results reported by the authors using the FLANN gave acceptable error of within 1% and an average CPU computation time of about 0.24s; also, the fuzzy ranking results showed that there are differences in collapse severity indices from the viewpoints of voltage deviation and voltage stability indicators.

In Man-Im et al (2019), a voltage stability margin called the L-index (Kessel & Glavitsch, 1986) is formulated into a minimization problem and integrated into a multi-objective optimal power flow solution for IEEE 30-bus power system including an active power generation source (wind power) cost and transmission power loss function. The L-index typically falls in the range of 0-1, and hence its minimization is very suitable for direct integration into most optimization functions. Chaotic mutation Stochastic Weight Trade-off (SWT) the swarm intelligence technique based on non-dominated sorting particle swarm optimization (NS-PSO), was then used for optimization. Using a crowding distance technique, the NS-PSO is able to improve the particle selection mechanism in PSO at the non-dominated front based on a neighbor density estimate. The results of simulations in the context of voltage stability (L-index) and in comparison, with various techniques indicate that NS-PSO will be the optimal one.

International Journal of Engineering Research & Technology (IJERT)
ISSN: 2278-0181
Vol. 10 Issue 05, May-2021

Wu et al. (2019) proposed an innovative multi-index solution for static voltage stability analysis (S-VSA) for power systems with renewable energy penetration (Wind Farms) in actual power grid in Hamil city, China. In their proposed multi-index solution, 6 stability indices (sub-criteria) were considered within 3 categorizations (called the primary criteria). An index weighting optimization strategy was proposed that combines subjective with objective importance weighting strategies; here, entropy weighting (EW) was employed for objective evaluation of variations in the considered indices and an Analytic Hierarchical Process (AHP) based on expert opinion was used to revise the objective weighting results. Furthermore, a Lagrange conditioned extreme value (LCEV) was employed to optimize a portion of index weights assigned by the objective and subjective techniques and a Fuzzy Order Preference by Similarity to Ideal Solutions (Fuzzy-TOPSIS) was used for performing realistic ranking of power system voltage buses. The results of simulation using the proposed approach indicate a similarity with other methods in the literature. In particular, the authors reported a sensitivity analysis which showed variation in wind farm performance for some indices while invariant behavior was observed for others. Thus, combination of indices may be a reasonable option in order to identify power system voltage states.

The phenomenon of large-scale blackouts – a situation of electrical system characterized by multiple simultaneous failure of different power sub-networks, has been investigated in Liu et al (2018). In their studies, 51 major blackouts across the world were reviewed, then the main causes summarized. Some of the studied countries were Northeastern USA, Canada, Western Australia, Barcelona in Spain, China etc.; some of the identified causes of cascaded blackouts include the Natural Causes (Thunderstorms, strong winds, earthquakes, Tsunamis), Failed Equipment (Transmission line and substation equipment – accounted for about 60% failure), Strategic Failure (lack of coordinated safety strategy – this cause is rare nowadays) and Manual Malfunction. Furthermore, they proposed a distributed accommodation/distributed energy within the context of energy internet (multi-energy interconnected system) to mitigate against blackouts. Such an approach encourages the use of energy hubs and alternate renewable sources of energy to support traditional grids and minimize dependency on a single source.

In Derafshian et al (2016), a multi-objective optimization load shedding scheme for the mitigation of voltage collapse in a section of Iran power system was proposed. The optimization approach uses a novel fuzzy-theta gravitational search algorithm based on optimal decision functions for securing the system. Their considered decision functions or multi-objectives are the Voltage Stability Margin (VSM), Total Load Cut (TLC) and Integral of the deviation from nominal voltage (IDNV). Also, six constraints were considered for the optimal solution; they include the Voltage Stability, Load Cut, the AC Power Flow, Active and Reactive Generation, Branch Maximum Flow and Voltage Magnitude constraints. Their technique was compared to three other similar multi-objective approaches and they reported improved performance over these methods based on a C-metric proposed earlier in (Zitzler & Thiele, 1999).

Ghahremani et al (2018) proposed very useful Special Protection Schemes (SPS) based on Local and Wide Area Networks (LWANs) for the Hydro-Quebec Power Transmission System. LWANS use telecommunication devices and phasor measurement units to support the global and local control of dynamic shunt compensators (GLCC) such as Static Var Compensators, STATCOMS etc used in maintaining the stability of the power system substation control unit (SCU).

III. METHODOLOGY

The methodology considered in this research considers the Line Voltage Stability Index (LVSI) proposed earlier in (Ratra et al., 2018), the predictive swarm particle intelligence (PSPI) comprising an Auditory Machine Intelligence (AMI) technique and a Particle Swarm Optimization (PSO) load flow solution technique provide in sub-sections 3.1, 3.2 and 3.3 respectively. The combined solution is also provided in sub-section 3.4.

1) Line Voltage Stability Index Estimation Model

The LVSI or Quadratic-LVSI (q- LVSI) model considers line charging capacitances and transmission line resistances a voltage collapse contingency calculation (Ratra et al., 2018). These two parameters were previously neglected by several techniques of Voltage Collapse Index (VCI).

The q-LVSI concept is as shown in Fig.1.

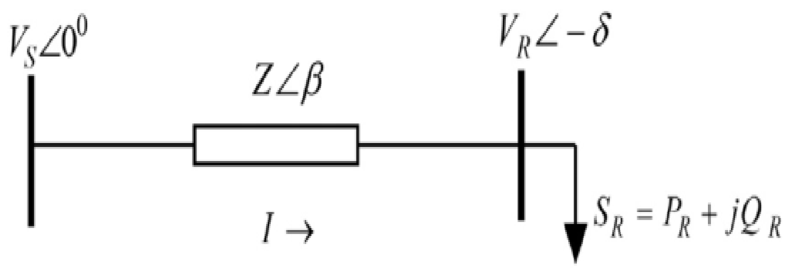

Fig.1. Concept of the q-LVSI used in this study (Source: Ratra et al., 2018).

The q-LVSI concept solution defines a sending end voltage, V_S, a receiving end voltage, V_R and a receiving power, S_R flowing through a transmission line characterized by an impedance, Z. The q-LVSI can be computed using eqn(1) as:

International Journal of Engineering Research & Technology (IJERT)
ISSN: 2278-0181
Vol. 10 Issue 05, May-2021

$$q-LVSI=\frac{2V_R A\cos(\beta-\alpha)}{V_S\cos(\beta-\delta)}>1 \quad (1)$$

From the ABCD representation, the V_S and I_s can take the following general forms:

$$V_s = AV_R + BI_R$$
$$I_s = CV_R + DI_R \quad (2)$$

where,

A→ 1 + Y*Z/2
B→ Z
C→ Y*(1+Y*Z/4), and
D→A.

This represents a complex-constant-representation where the parameters A and D do not change and B and C are complex variables.

At zero loading, the current flow $I_R = 0$. This implies:

$V_s = AV_R, (\delta_s) = 0, V_r(\delta_r) = 0$

and

q-LVSI = 2, which is the most stable condition.

In practice, the q-LVSI upper-bound may exceed stated theoretical limits. In this research, we using a signal conditioning formula based on a logical inversion rule as in eqn(3):

$$q-LVSI=\begin{cases}\left[Not\left(q-LVSI\right)>2\right]\cdot q-LVSI, q-LVSI>2\\ q-LVSI, 0<q-LVSI<2\end{cases} \quad (3)$$

Full details of the mathematical calculations to arrive at this index can be found in (Ratra et al., 2018) and in (Idoniboyeobu et al., 2018).

2) Auditory Machine Intelligence Technique

Auditory Machine Intelligence (AMI) is basically a deterministic machine intelligence neural technique that was introduced in (Osegi & Anireh, 2016) under the name "Deviant Learning Algorithm for time series prediction. This technique was further developed in (Osegi & Anireh, 2020) to overcome the limitations in the temporal learning phase of Hierarchical Temporal Memory (HTM) neural techniques developed in (Cui et al., 2016; Cui et al., 2017; Osegi, 2018). AMI exploits the idea and findings about the mismatch negativity effect (MMN) and intelligent processing in mammalian auditory cortex to build an algorithm that gives more precise predictions in a timely and more reliable manner. The MMN is a differential neuronal response to a repetition of stimulus presentations and an oddball or deviant stimulus signal (Takaura & Fujii, 2016). MMN has also been shown to exhibit very important high level cognitive processes (Näätänen et al., 2007). Thus the AMI principle is based on the MMN theory (Takaura & Fujii, 2016; Näätänen et al., 2007; Näätänen et al., 1978; Lieder et al., 2013a; Lieder et al., 2013b) and the theory of functional reorganization in mammalian auditory cortex (Sollini et al., 2018).

The AMI algorithm is as described in Algorithm 1. It basically occurs in two-phases (Osegi and Anireh, 2020; Osegi et al., 2018):

- A Phase-1 or low-level prediction for making a prediction in the current time step based on a history of sparse data points in the previous time step. These sparse data points correspond to the evoked potentials originally observed in (Näätänen et al., 1978) as the "odd-ball".
- A Phase-2 or high-level prediction that performs look-ahead predictions several time steps ahead.

In the proposed voltage collapse prediction system, a Phase-1 prediction is used to perform single or one-step-ahead forecasts of streaming power loads. The AMI performs this operation using the computation of a single learning formula and no specific random fine-tuning is needed to learn on the data. In phase-1 predictions, the AMI learns a sequence of data points (values) automatically/temporally in an adaptive manner such that a mean deviant point is computed as in (4):

$$S_{dev(mean)}=\frac{\left(\left(\frac{\sum\left[S_{dev}\right]}{(n-1)}\right)+S_{deviant}\right)-2}{n+1} \quad (4)$$

where,
n = number of data points in a temporal sequence
$S_{deviant}$ = the *(n-1)th* value of the temporal sequence
S_{dev} = the difference between $S_{deviant}$ and S_{stars}
S_{stars} = the *(n-2)th* values of the temporal sequence
S^* = sparse set of input sequences

In order to make a prediction with the AMI, the formula in (5) is used as:

$$S_{pred}=S_{deviant}+S_{dev(mean)} \quad (5)$$

International Journal of Engineering Research & Technology (IJERT)
ISSN: 2278-0181
Vol. 10 Issue 05, May-2021

where,

$$S_{deviant} = S_n^* - 1 \tag{6}$$

$$S_{stars} = S_n^* - 2 \tag{7}$$

Algorithm 1. AMI Processing Algorithm

1: Initialize S_{pred}, as prediction parameter, S_{stars}, as input sequences (standards) State, $S_{dev(mean)}$ as deviant mean, j as iteration counter.

2: *for* all s $\in$ $s.S_{stars}$, && $j > 1$, do

3: Compute $S_{deviant}$ and S_{stars} using equations (6) and (7)

4: $S_{dev} \leftarrow \| S_{deviant} - S_{stars} \|$ // deviations from standards

5: Compute $S_{dev(mean)}$ using equations (4)

6: Compute S_{pred} using equations (4) and (6)

7: Update $S_{dev(mean)}$ using Algorithm 2

8: *end for*

The AMI algorithm also uses a hebbian learning rule as follows: if the current prediction error of the AMI neuron is greater than or lower than zero, we reinforce its prediction by decreasing or increasing its deviant weight value by the absolute prediction error difference at the current time step; otherwise we perform zero or negligible positive reinforcement by adding a very small value (deviant-laplacian correction). In the case where exact matches occur, a small laplacian correction value (typically in small fractions of about a hundredth), is used for deviant weight updates. The learning rule is described succinctly in Algorithm 2.

Algorithm 2. AMI Learning Algorithm

1: Initialize S_{pred}, as prediction parameter, S_{stars}, as input sequences (standards) State, $S_{dev(mean)}$ as deviant mean, $S_{diff(1)}$ as difference between S_{pred}, $S_{deviant}+1$ and $S_{diff(2)}$ as difference between $S_{dev(mean)}$ and $|S_{diff(1)}|$, l_p as correction factor or bias.

2: *for* all s $\in$ $s.S_{stars}$ do

3: if $S_{diff(2)} > 0$

4: $S_{dev(mean)} \leftarrow S_{dev(mean)} - |S_{diff\ (1)}|$ // Weaken deviant mean by a factor, $|S_{diff(1)}|$

5: elseif $S_{diff(2)} < 0$

6: $S_{dev(mean)} \leftarrow S_{dev(mean)} + |S_{diff\ (1)}|$ // Reinforce deviant mean by a factor, $|S_{diff(1)}|$

7: else

8: $S_{dev(mean)} \leftarrow S_{dev(mean)} + l_p$

9: end if

10: *end for*

Source: (Idachaba, et. al., 2020)

International Journal of Engineering Research & Technology (IJERT)
ISSN: 2278-0181
Vol. 10 Issue 05, May-2021

3) Particle Swarm Optimization Load Flow Technique

In most typical voltage collapse strategies, the Load Flow Analysis (LFA) play an integral part in the identification and calculation of the required core parameters (bus voltages and angles in the case of q-LVSI) needed for deriving the stability indices. The Swarm Particle Optimizer (SPO) is one very useful alternative strategy for solving a power network. The concept behind swarm particles was first introduced by Kennedy and Eberhart (Kennedy & Eberhart, 1995). It involves the determination of a particles new solution vector (new velocity state) from a population of particles in a well defined random manner. The randomization step is typically influenced by a continual update of a weighted velocity vector in addition to a randomized position state – the states being a sum of the difference between random previous best position states with previous (initial) states at both local and global levels (Sumathi & Surekha, 2010). This operation follows a somewhat Newtonian representation as described by the velocity update calculation in eqn(8):

$$\begin{aligned} vel_{ij}(new) &= w * vel_{ij}(old) + c_1 rand_1\left(pbest_{ij}(old)\right) \\ &- pos_{ij}(old) + c_2 rand_2\left(pbest_{ij}(old)\right) - pos_{ij}(old) \end{aligned} \quad (8)$$

The new position is also updated by adding the velocity update obtained in eqn(3.11) to its old position as in eqn(9):

$$pos_{ij}(new) = pos_{ij}(old) + vel_{ij}(new) \quad (9)$$

where,

$rand_1$, $rand_2$ = random number between 0 and 1

w = inertia weight

c_1 = coefficient of self-recognition

c_2 = social coefficient

c_1, c_2 = 2.

Basically, the procedure for an SPO solution is as shown in Algorithm 3 (Sumathi & Surekha, 2010):

Algorithm 3. The Swarm Particle Optimizer Algorithm

Initialize the size of the swarm particles, *n*

Randomly initialize swarm particle position, *x* and velocities, *v*

While stopping criterion is false **do**

t = t+1

Compute fitness value of each particle

$$x* = \arg\min_{t-1}^{n}\begin{pmatrix} f\left(x*(t-1)\right), f\left(x_1(t)\right), \\ f\left(x_2(t)\right), \ldots f\left(x_t(t)\right), \ldots f\left(x_n(t)\right) \end{pmatrix};$$

For *i*=1 to n

$$x_t^{\#}(t) = \arg\min_{t-1}^{n}\left(f\left(x_t^{\#}(t-1)\right), f\left(x_t(t)\right)\right)$$

For *j* = 1 to Dimension

Update the jth dimension of x_t and v_t //x_t = *pos*, v_t = *vel*

Execute eqn(8)

Execute eqn(9)

End For

End For

End While

When applying particle swarm approach to a power systems Load Flow Analysis (LFA) problem, the power system design variables to be optimized (bus voltages and angles, real and reactive powers etc) are described as position vectors and are typically constrained within an upper/lower bound. The parameters to be solved will require the definition of the real and reactive power injections from real operation stations and the calculation of the real and reactive powers based on the network transmission line parameters.

The power mismatch models in eqn(10) and eqn(11) describes the aforementioned operation which is required in an SPO objective function. The primary purpose is to minimize this objective over all differential summations of the power mismatches such that it is less than a stated permissible error value defined by a value say, ε as in (12).

$$\Delta P_i = P^{inj} - \sum_{j=1}^{n}|V_i||V_j||Y_{ij}|\cos\left(\delta_i - \delta_j - \theta_{ij}\right) \quad (10)$$

$$\Delta Q_i = Q^{inj} - \sum_{j=1}^{n}|V_i||V_j||Y_{ij}|\sin\left(\delta_i - \delta_j - \theta_{ij}\right) \quad (11)$$

$$obj+ = \min\left\{|\Delta P_i|, |\Delta Q_i|\right\} \leq \varepsilon \qquad \forall i \tag{12}$$

where,

ΔP_i = active power mismatches at bus i

ΔQ_i = reactive power mismatches at bus i

P^{inj} = injected active power at bus i

Q^{inj} = injected reactive power at bus i

$|V_i|$ = absolute value of the complex voltage at bus i

$|V_j|$ = absolute value of the complex voltage at bus j

$|Y_{ij}|$ = absolute value of the admittance matrix of the *ijth* element

θ_{ij} = admittance angle at bus i, j

δ_i = voltage angle of the bus i

δ_j = voltage angle of the bus j

ε = stopping criterion

The concept flow chart for SPO Load Flow Analysis (LFA) prior to voltage collapse indexing is as shown in Fig.2. A generalized q-LVSI solution incorporating the functionality of SPO is also shown in Fig.3.

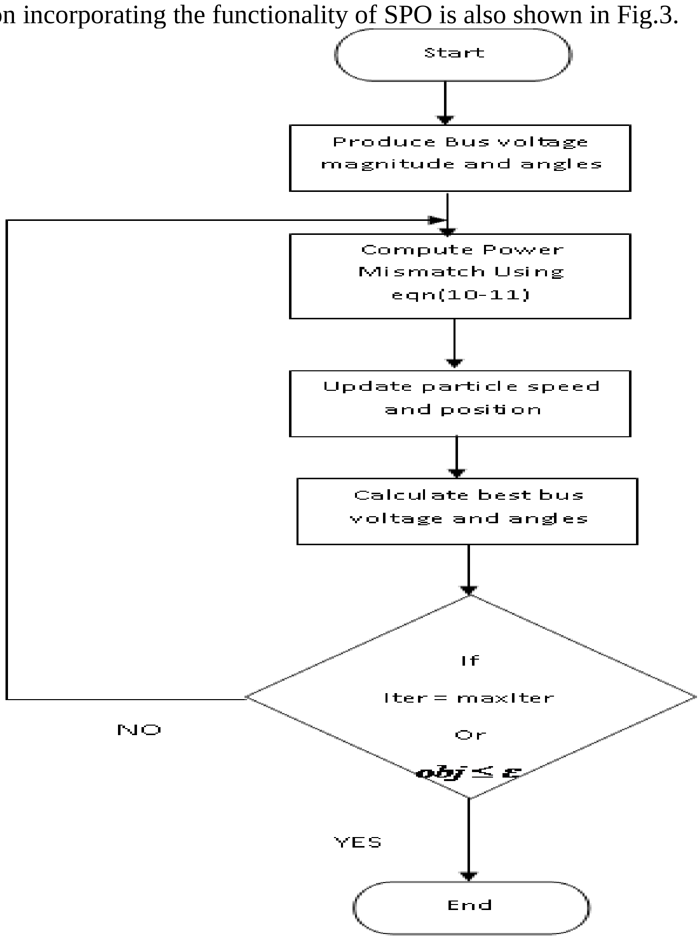

Fig.2. PSO Load Flow concept

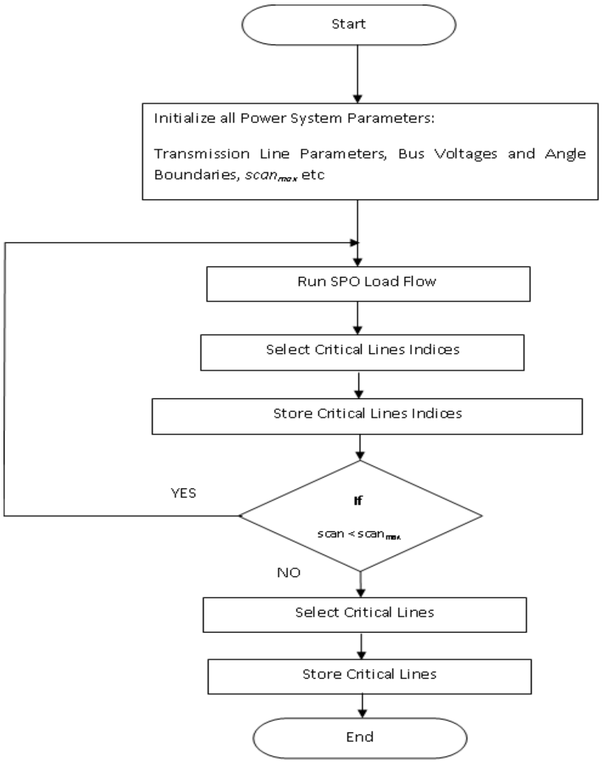

Fig.3. Generalized q-LVSI base technique

4) Combined systems solution

The combined AMI prediction layer and the PSO with the existing q-LVSI estimator model add neuro-swarm capabilities to the voltage collapse index estimation system. In this study, an online (continual) voltage-stability-indexing scheme is employed for analyzing the voltage collapse state of a topology of the existing 330-kV Nigerian Power network. The developed scheme is diagrammatically described in the flowchart of Fig.4. The power-stability-indexing scheme is operated in an online mode hopefully improving its prediction performance as the number of trial passes (scans) of the AMI predictor is increased.

International Journal of Engineering Research & Technology (IJERT)
ISSN: 2278-0181
Vol. 10 Issue 05, May-2021

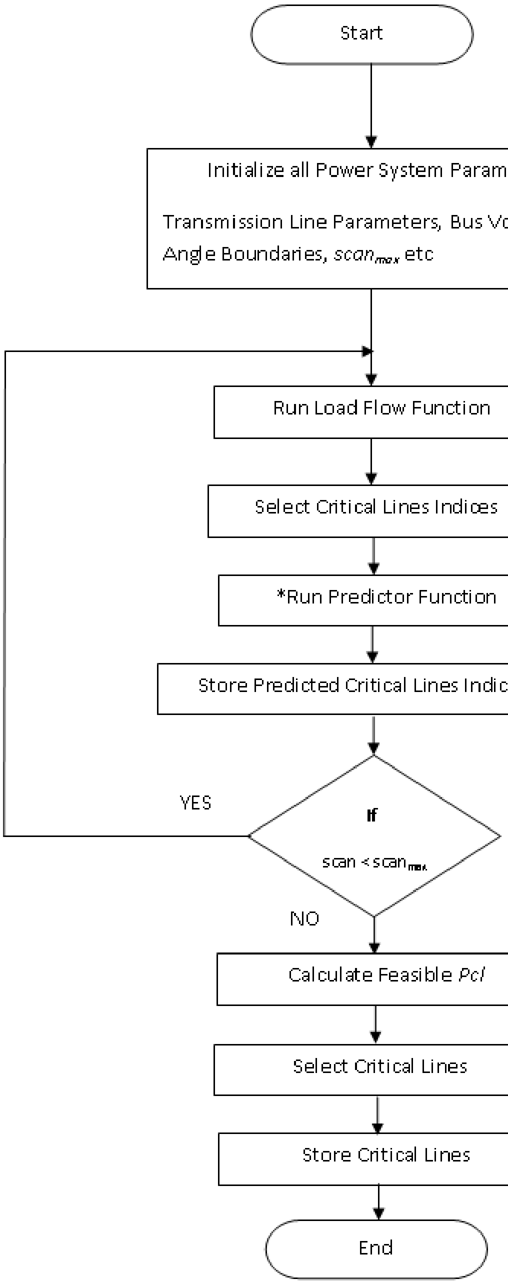

Fig.4. *q*-LVSI Predictor technique

IV. DISCUSSIONS

The experimental results using the proposed PSPI technique for voltage collapse studies of Nigerian 330kV, 11-machine, 34-bus power network are reported in this section. Specifically, vulnerability of existing lines in terms of the q-LVSI-Predictor including a determination of the critical lines and the most critical line in the study network are investigated and reported. The line data, bus data and power system generation and load data used in the analysis can be found in (Ikeli, 2009); for clarity in interpretation, these data are provided in the Appendix. The compensation experiments requires the use of a shunt MVARs of between 0 and 50MVARs for the VSM improvement. The SPO part requires that the population size be set to 20 and the iteration steps set to 100. Constriction coefficients and damping factors are also 2.05 and 1.0 respectively. All simulations have been performed in the MATLAB environment using an Intel i-core-3 processor board.

1) Experiments with the 11-machine 34-bus Nigerian 330-kV Power System Network

The experimental the results of experiments using the proposed q-LVSI-Predictor are presented considering a fixed reactance loading and a well defined number of scan cycles. The system is developed based on the quadratic Line Voltage Stability Index (q-LVSI) index, the Swarm Particle Optimizer (SPO) load flow, and the Auditory Inspired Machine Intelligence technique (AIMI) described earlier in Section 3. The system settings are based on data provided earlier in (Ikelli, 2009) and are given in Appendix A (Tables A.1-A.3). An additive reactance loading of 2.0.p.u on all PQ buses is also defined. The systems simulation experiments are performed in the MATLAB programming environment and are conducted for two different scan cycles (main program repeats) of 10 and 50 scans provided in sub-sections 4.1.1and 4.1.2 respectively.

International Journal of Engineering Research & Technology (IJERT)
ISSN: 2278-0181
Vol. 10 Issue 05, May-2021

a) Voltage Collapse Study Experiments using 10 scans

The results of q-LVSI-Predictor for 10 scans are as shown in Tables 1-2. This includes results for the predicted and actual indexes of the line and the predicted critical lines.

Table.1. Predicted and actual values of the q-LVSI line sequence indexes for 10 scans

s.n.	Predicted Line Index Sequence	Expected Line Index Sequence
1	46	35
2	-4	1
3	17	15
4	43	35
5	1	3
6	2	3
7	2	3
8	31	27
9	35	31

Table.2. Predicted Critical Lines for 10 scans

From	To
14	17
1	2
1	4
1	4
22	29
24	25

From the Table 2, it is obvious that the most frequent critical line is Lines 1-4 which correspond to buses Kainji-GS to Jebba-TS. The mean absolute percentage error (mape) in this prediction was found to be 0.288; the online error response as computed from the AMI algorithm predictions is as shown in Fig.5.

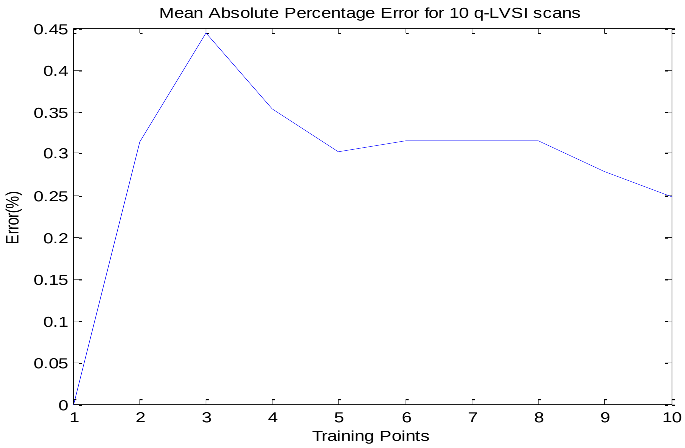

Fig.5. Online (Continual) Training Error Response of q-LVSI AMI Predictor (10 scans)

b) Voltage Collapse Study Experiments using 50 scans

The results of q-LVSI-Predictor for 50 scans are as shown in Tables 3-4. This includes results for the predicted and actual indexes of the line and the predicted critical lines.

Table.3. Predicted and actual values of the q-LVSI line sequence indexes for 50 scans

S/N	Predicted Line Index Sequence	Expected Line Index Sequence
1	3	3
2	3	3
3	2	2
4	3	3
5	3	3

International Journal of Engineering Research & Technology (IJERT)
ISSN: 2278-0181
Vol. 10 Issue 05, May-2021

6	1	1
7	2	2
8	36	31
9	17	15
10	31	27
11	0	1
12	0	1
13	30	27
14	0	1
15	38	35
16	0	1
17	1	1
18	16	15
19	1	1
20	29	27
21	16	15
22	16	15
23	3	3
24	16	15
25	1	1
26	1	1
27	33	31
28	3	3
29	1	1
30	28	27
31	3	3
32	32	31
33	28	27
34	15	15
35	37	35
36	3	3
37	1	1
38	1	1
39	15	15
40	3	3
41	1	1
42	2	2
43	1	1
44	15	15
45	3	3
46	3	3
47	15	15
48	1	1
49	32	31

Table.4. Predicted Critical Lines for 50 scans

From	To
3	4
3	4
1	4
3	4
3	4
1	2
1	4
28	29
14	17
22	29
22	28
33	34
1	2

International Journal of Engineering Research & Technology (IJERT)
ISSN: 2278-0181
Vol. 10 Issue 05, May-2021

12	15
1	2
19	27
12	15
12	15
3	4
12	15
1	2
1	2
23	31
3	4
1	2
19	26
3	4
23	30
19	26
11	15
32	33
3	4
1	2
1	2
11	15
3	4
1	2
1	4
1	2
11	15
3	4
3	4
11	15
1	2
23	30

From the Table 4, the most frequent critical lines are Lines 1-2 and 3-4 corresponding to bus interconnections: Kainji-GS-to-Bernin-Kebbi and Jebba-GS-to-Jebba-TS respectively. The mean absolute percentage error (mape) in this prediction was found to be 0.0841; the online error response as computed from the AMI algorithm predictions is as shown in Fig.6.

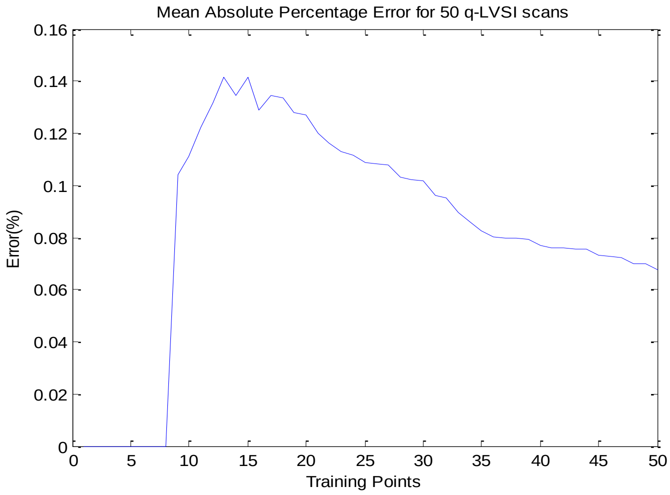

Fig.6. Online (Continual) Training Error Response of q-LVSI AMI Predictor (50 scans)

V. CONCLUSIONS

In this research, the promising directions of the Swarming AI technique called SPIP for Swarm Particles Intelligence, combined with an emerging machine intelligence neural technique, the AMI has been presented for the case of voltage collapse studies in Nigerian 330kV 34-bus Power Network. The emphasis of this was to evaluate the effectiveness of swarm-predictive technique for determining the critical and most critical lines that may suffer a voltage collapse in the Nigerian power transmission system.

International Journal of Engineering Research & Technology (IJERT)
ISSN: 2278-0181
Vol. 10 Issue 05, May-2021

This includes employing a swarm based load flow solution and a neural LVSI prediction technique that improves through time or sequential expansion.

The results show that using this approach, it is possible to determine the critical buses in a power network at improved accuracies depending on the number of SPIP program trial run simulations. It is also possible that there will be further improvements in prediction error accuracies and the identification of more stable line predictions as the number of trial run simulations is increased. Thus, power system operators can leverage this approach to plan ahead of any unforeseen contingency to secure the most voltage-collapse critical parts of the power system network.

VI. REFERENCES

[1] Cui, Y., Ahmad, S., & Hawkins, J. (2016). Continuous online sequence learning with an unsupervised neural network model. *Neural computation*, *28*(11), 2474-2504.

[2] Cui, Y., Ahmad, S., & Hawkins, J. (2017). The HTM spatial pooler—A neocortical algorithm for online sparse distributed coding. *Frontiers in computational neuroscience*, *11*, 111.

[3] Derafshian, M., Amjady, N., & Dehghan, S. (2016). Special protection scheme against voltage collapse. *IET Generation, Transmission & Distribution*, *10*(2), 341-351.

[4] Dobson, I., & Lu, L. (1993). New methods for computing a closest saddle node bifurcation and worst case load power margin for voltage collapse. *IEEE Transactions on Power Systems*, *8*(3), 905-913.

[5] Ghahremani, E., Heniche-Oussedik, A., Perron, M., Racine, M., Landry, S., & Akremi, H. (2018). A detailed presentation of an innovative local and wide-area special protection scheme to avoid voltage collapse: From proof of concept to grid implementation. *IEEE Transactions on Smart Grid*, *10*(5), 5196-5211.

[6] Hole, K. J., & Ahmad, S. (2019). Biologically Driven Artificial Intelligence. *Computer*, *52*(8), 72-75.

[7] Idoniboyebu, D. C., Braide, S. L., & Idachaba, A. O. (2018). Analysis of Voltage Collapse in the Nigeria 30 Bus 330kv Power Network. *IOSR Journal of Electrical and Electronics Engineering (IOSR-JEEE)*, *13*(4), 42-50.

[8] Ikeli, H. N. (2009). A Critical Analysis of Transient Stability of Electrical Power System A Case Study of Nigerian 330kv Power System. MEng. Thesis, University Of Nigeria, Nsukka.

[9] Kennedy, J., & Eberhart, R. (1995, November). Particle swarm optimization (PSO). In *Proc. IEEE International Conference on Neural Networks, Perth, Australia* (pp. 1942-1948).

[10] Kessel, P., & Glavitsch, H. (1986). Estimating the voltage stability of a power system. *IEEE Transactions on power delivery*, *1*(3), 346-354.

[11] Lieder, F., Daunizeau, J., Garrido, M. I., Friston, K. J., & Stephan, K. E. (2013). Modelling trial-by-trial changes in the mismatch negativity. *PLoS Comput Biol*, *9*(2), e1002911.

[12] Lieder, F., Stephan, K. E., Daunizeau, J., Garrido, M. I., & Friston, K. J. (2013). A neurocomputational model of the mismatch negativity. *PLoS Comput Biol*, *9*(11), e1003288.

[13] Liu, B., Zhou, B., Jiang, D., Yu, Z., Yang, X., & Ma, X. (2018). Distributed Accommodation for Distributed Generation–From the View of Power System Blackouts. In *Advances in Green Energy Systems and Smart Grid* (pp. 236-246). Springer, Singapore.

[14] Man-Im, A., Ongsakul, W., Singh, J. G., & Madhu, M. N. (2019). Multi-objective optimal power flow considering wind power cost functions using enhanced PSO with chaotic mutation and stochastic weights. *Electrical Engineering*, 1-20.

[15] Näätänen, R., Gaillard, A. W., & Mäntysalo, S. (1978). Early selective-attention effect on evoked potential reinterpreted. *Acta psychologica*, *42*(4), 313-329.

[16] Näätänen, R., Paavilainen, P., Rinne, T., & Alho, K. (2007). The mismatch negativity (MMN) in basic research of central auditory processing: a review. *Clinical neurophysiology*,*118*(12), 2544-2590.

[17] Osegi, E. N., & Anireh, V. I. (2016). Deviant Learning Algorithm: Learning Sparse Mismatch Representations through Time and Space. *arXiv preprint arXiv:1609.01459*.

[18] Osegi, E. N. (2020). Using the hierarchical temporal memory spatial pooler for short-term forecasting of electrical load time series. *New England Journal of Entrepreneurship,* Vol. ahead-of-print No. ahead-of-print. https://10.1016/j.aci.2018.09.002.

[19] Osegi, E. N., Anireh, V. I., & Onukwugha, C. G. (2018, June). pCWoT-MOBILE: a collaborative web based platform for real time control in the smart space. iSTEAMS SMART-MIINDs Conference, *13*(3), 237-250

[20] OSEGİ, E. N., & ANİREH, V. I. (2020). AMI: An Auditory Machine Intelligence Algorithm for Predicting Sensory-Like Data. *Bilgisayar Bilimleri*, *5*(2), 71-89.

[21] Prasad, M., Puhan, S. S., & Patra, S. (2019, January). Contingency Selection in the Context of Voltage Security Margin Determination. In *International Conference on Intelligent Computing and Communication Technologies* (pp. 744-752). Springer, Singapore.

[22] Ratra, S., Tiwari, R., & Niazi, K. R. (2018). Voltage stability assessment in power systems using line voltage stability index. *Computers & Electrical Engineering*, *70*, 199-211.

[23] Sollini, J., Chapuis, G. A., Clopath, C., & Chadderton, P. (2018). ON-OFF receptive fields in auditory cortex diverge during development and contribute to directional sweep selectivity. *Nature communications*, *9*(1), 1-12.

[24] Sumathi, S., & Paneerselvam, S. (2010). *Computational intelligence paradigms: theory & applications using MATLAB*. CRC Press.

[25] Takaura, K., & Fujii, N. (2016). Facilitative effect of repetitive presentation of one stimulus on cortical responses to other stimuli in macaque monkeys–a possible neural mechanism for mismatch negativity. *European Journal of Neuroscience*, *43*(4), 516-528.

[26] Wu, J., Wang, H., Yao, L., Kang, Z., & Zhang, Q. (2019). Comprehensive evaluation of voltage stability based on EW-AHP and Fuzzy-TOPSIS. *Heliyon*, *5*(10), e02410.

[27] Zitzler, E., & Thiele, L. (1999). Multiobjective evolutionary algorithms: a comparative case study and the strength Pareto approach. *IEEE transactions on Evolutionary Computation*, *3*(4), 257-271.

International Journal of Engineering Research & Technology (IJERT)
ISSN: 2278-0181
Vol. 10 Issue 05, May-2021

Appendix A: Power system parameters

Table A.1: Nomenclature of the 34 bus 11-Machine Power Network

Bus No.	Bus Code*	Type of Bus	Bus Name
1	1	Slack	Kainji G.S
2	0	PQ	Bernin Kebbi
3	2	PV	Jebba G.S
4	0	PQ	Jebba T.S
5	0	PQ	Shiroro T.S
6	0	PQ	Abuja(katampe)
7	2	PV	Shiroro G.S
8	0	PQ	Ayede T.S
9	0	PQ	Oshogbo T.S
10	0	PQ	Kaduna T.S
11	2	PV	Olorunsongo G.S
12	0	PQ	Sakete T.S
13	0	PQ	Kano T.S
14	0	PQ	Jos T.S
15	0	PQ	Ikeja West T.S
16	0	PQ	Benin T.S
17	0	PQ	Gombe T.S
18	2	PV	Delta G.S
19	0	PQ	Ajaokuta T.S
20	0	PQ	Akangba T.S
21	0	PQ	Omotosho T.S
22	2	PV	Egbin G.S
23	0	PQ	Onitsha T.S
24	2	PV	Sapele G.S
25	0	PQ	Aladja T.S
26	2	PV	Geregu G.S
27	2	PV	Ascon G.S
28	2	PV	AES G.S
29	0	PQ	Aja T.S
30	0	PQ	New Heaven T.S
31	2	PV	Okpai G.S
32	0	PQ	Alaoji T.S
33	2	PV	Afam G.S
34	2	PV	Omoku G.S

Table A.2: Transmission Line Parameters

From	To	R(p.u)	X(p.u)	B(p.u)	Tap
1	2	0.0122	0.0916	1.2100	1
1	4	0.0016	0.0120	0.3100	1
3	4	0.0002	0.0094	0.0000	1
4	5	0.0048	0.0360	0.0900	1
4	9	0.0021	0.0155	0.0700	1
5	6	0.0019	0.0142	0.3600	1
5	7	0.0003	0.0188	0.0000	1
5	10	0.0019	0.0142	0.3700	1
8	9	0.0054	0.0405	0.3300	1
8	15	0.0053	0.0406	0.4500	1
9	15	0.0065	0.0427	0.5500	1
9	16	0.0099	0.0742	0.9800	1
10	13	0.0090	0.0680	0.5200	1
10	14	0.0077	0.0582	0.7700	1
11	15	0.0021	0.0104	0.3100	1
12	15	0.0041	0.0305	0.4100	1
14	17	0.0104	0.0783	0.0100	1
15	16	0.0110	0.0828	0.0900	1

15	20	0.0004	0.0027	0.0500	1
15	21	0.0055	0.0414	0.3500	1
15	22	0.0012	0.0092	0.2000	1
16	18	0.0064	0.0405	0.1500	1
16	19	0.0038	0.0288	0.7600	1
16	21	0.0055	0.0414	0.5500	1
16	23	0.0054	0.0405	0.3800	1
16	24	0.0010	0.0074	0.1900	1
18	25	0.0010	0.0077	0.1000	1
19	26	0.0005	0.0038	0.3800	1
19	27	0.0006	0.0038	0.4000	1
22	28	0.0005	0.0036	0.3000	1
22	29	0.0003	0.0021	0.2000	1
23	30	0.0038	0.0284	0.3700	1
23	31	0.0049	0.0037	0.0900	1
23	32	0.0061	0.0455	0.0200	1
24	25	0.0025	0.0186	0.2400	1
28	29	0.0035	0.0206	0.3000	1
32	33	0.0010	0.0074	0.0900	1
33	34	0.0005	0.0038	0.3000	1

Table A.3: System Loading Data including PV generation and PQ-Loading

Bus No.	MW	MVAR
1	520	--
2	40	-10
3	300	110(0)
4	140	30
5	90	30
6	160	70
7	400	140(0)
8	130	70
9	300	90
10	210	40
11	150	114(0)
12	50	-20
13	100	-30
14	120	60
15	500	50
16	250	43
17	70	38
18	280	100(0)
19	200	55
20	150	35
21	240	104(0)
22	700	108(0)
23	300	45
24	180	132(0)
25	100	58
26	190	126(0)
27	150	100(0)
28	130	150(0)
29	120	80
30	130	-78
31	150	100(0)
32	200	67
33	200	140
34	300	125